The Institution of Engineering and Technology

The Institution of Engineering and Technology

PEMD 2014
Conference on Power Electronics, Machines and Drives

8 - 10 April 2014 | Midland Hotel, Manchester, UK

Tuesday 8 April 2014

0166 **DAG SVM and pitch synchronous wavelet transform for induction motor diagnosis**
H Keskes[1], A Braham[1,2], [1]*INSAT, Tunisia,* [2]*Carthage University, Tunisia*

0175 **ANN-based system for discrimination between unbalanced supply voltage and phase loss in induction motors**
S Refaat[1], H Rub[1], A Iqbal[2], [1]*Texas A&M university at Qatar, Qatar,* [2]*Qatar University, Qatar*

0229 **A novel FCS-model predictive control algorithm with duty cycle optimization for surface-mounted PMSM**
S Wang[1], C Xia[1,2], X Gu[2], W Chen[1], [1]*Tianjin University, China,* [2]*Tianjin Polytechnic University, China*

0230 **Evaluation of SVM speed and position observers for sensorless PMSM in start-up region**
X Lu[1], H Lin[1], Y Feng[1], Y Guo[1], H Yang[1], Y Zhang[1], [1]*Southeast University, China*

0238 **Hysteresis-based DIFC in SRM: eliminating switching harmonics while improving inverter efficiency**
A Hofmann[1], R W De Doncker[1], [1]*Institute for Power Electronics and Electrical Drives, Germany*

0249 **A novel multi-level electro-mechanical actuator virtual testing and analysis tool**
P Giangrande[1], C Hill[1], S Bozhko[1], C Gerada[1], [1]*University of Nottingham, UK*

0272 **Determination of the cogging torque sensitivity of brushless permanent magnet machines due to changes of the material characteristics of ferromagnetic components**
G Bramerdorfer[1], P Gangl[2], A Fohler[1], U Langer[2], W Amrhein[1], [1]*Johannes Kepler University, Austria,* [2]*Institute of Computational Mathematics, Austria*

0315 **Parametric, self-segmenting mesh generation tool for the steady state thermal estimation of induction machines**
C Bednar[1], S A Semidey[1], J R Mayor[1], [1]*Georgia Institute of Technology, USA*

0324 **Load point calculation for low voltage synchronous generator using finite element method**
A Fernandez[1,2], D Prieto[1,2], J Vannier[1], P Manfe[2], J Saint-Michel[2], [1]*Supélec, France,* [2]*Leroy Somer, France*

0328 **Simulation and optimisation of a Flux-Switching Machine with large air-gap using finite element method**
A Lindner[1], I Hahn[1], [1]*University of Erlangen-Nuremberg, Germany*

0332 **Thermal equivalent circuit for outer rotor type motors**
K Kim[1], H Kim[1], H Hong[1], [1]*Hanyang University, Republic of Korea*

0356 **On-line diagnosis of high-resistance connection for inverter fed induction motors**
P de la Barrera[1], R Leidhold[2], G Bossio[1], [1]*Universidad Nacional de Río Cuarto, Argentina,* [2]*Otto-von-Guericke-Universität Magdeburg, Germany*

Thermal Equivalent Circuit Network for Outer Rotor Type Motors

K S Kim, H J Kim, J P Hong

Department of Automotive Engineering, Hanyang University, Seoul 133-791, Korea

Keywords: convection, conduction, thermal equivalent circuit, thermal test

Abstract

In the industry and military field, hydraulics is substituted by motor. In contrast with automotive and home appliance, this motor required various torque level. The test motor operates under low speed and high torque. Because this motor needed high armature current and armature is located in near shaft in the outer rotor type, this is disadvantage than inner rotor type in the radiant. In this paper, the thermal analysis is conducted by thermal equivalent circuit, analysis is compared with test.

1 Introduction

Interest in interior permanent magnet synchronous motors (IPMSM) has been growing because high torque and a wide speed range can be achieved by flux weakening of the current vector control [1,2]. Because of these advantages, IPMSM is widely used in many area; home application, automotive engineering, and military etc.

In the IPMSM, several considerations exist by a material as a necessity. For example, thermal problem is critical consideration which is influenced by the heat source. In the operation, losses which contain copper loss, core loss, and eddy current loss in the permanent magnet is generated. These losses are increase without method of radiant heat, electric breakdown and irreversible demagnetization are generated in winding and permanent magnet. In addition, desired life time decreases. For preventing negative effect and determining the maximum rating, thermal analysis is necessary.

In the outer rotor type motor, stator is located in near shaft. If the motor operates in the low speed and high torque, copper loss is larger than core loss. In this case, copper loss which is generated in the stator winding is influence the motor temperature. Therefore, thermal analysis and estimation is essential in the outer rotor type motor [3].

In this paper for estimation of thermal temperature, thermal equivalent circuit network is adopted. The equivalent circuit has several advantage comparing the computational fluid dynamics (CFD). The thermal circuit is easy to analysis because equivalent model mathematically concise, equivalence and solving time is very short than CFD. In addition, difference between test and analysis value is very small. Therefore, using thermal equivalent circuit network, outer rotor type motor is analyzed.

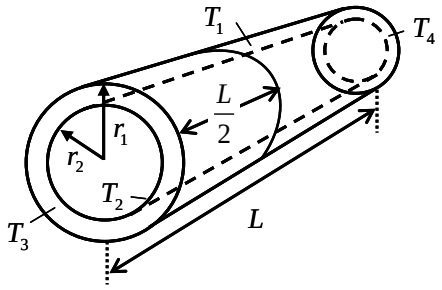

Figure 1: Equivalent model of motor considering cylindrical shape.

2 Component of thermal equivalent circuit

Thermal equivalent circuit network is composed of several parameter; thermal resistance, heat source, thermal capacitance. The thermal resistance is divide by conduction and conduction. The heat source is loss which is generated to core, coil, and permanent magnet. The thermal capacitance is the capacity. In this chapter, these parameters are dealt with in detail.

2.1 Thermal resistance of the conduction

When the heat due to motor loss is applied to each part, the conduction is generated. Because the coefficient is larger than convection, this heat transfer is more rapid than convection. This resistance is easy to design if motor is divided to several part. The core is divided to radial direction and axial direction. The thermal resistance is obtained by

$$R_{cond} = \frac{l}{kA} \qquad (1)$$

where k is coefficient of conductive heat transfer, A is the area through the heat, l is the length. This is base equation for obtaining the each direction. Fig.2 shows the modeling of the mal resistance at yoke. In the radial direction, (2) and (3) are

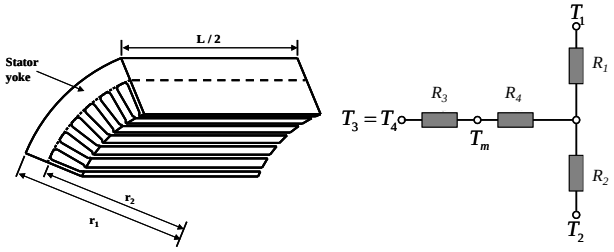

Figure 2: Modeling of thermal resistance at yoke.

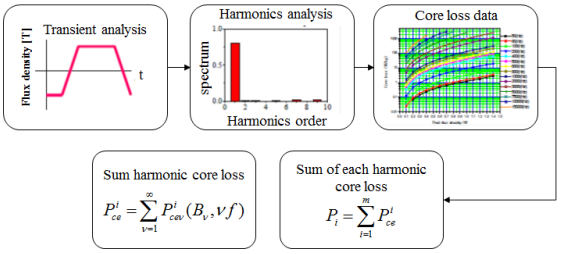

Figure 3: Calculation process of core loss.

applied, (4) is applied to axial direction. In the lumped parameter method, (5) is the compensating resistance between mean and peak temperature [4,5].

$$R_3 = \frac{1}{2\pi k_r Ls}\left[1-\left(2r_2^2 \ln\left(\frac{r_1}{r_2}\right)\right)/\left(r_1^2 - r_2^2\right)\right] \quad (2)$$

$$R_4 = \frac{1}{2\pi k_r Ls}\left[\left(2r_1^2 \ln\left(\frac{r_1}{r_2}\right)\right)/\left(r_1^2 - r_2^2\right) - 1\right] \quad (3)$$

$$R_1 = \frac{L}{6\pi k_a (r_1^2 - r_2^2)} \quad (4)$$

$$R_2 = \frac{-1}{4\pi k_r Ls (r_1^2 - r_2^2)} \cdot \left[r_1^2 + r_2^2 - \left(4r_1^2 r_2^2 \ln\left(\frac{r_1}{r_2}\right)\right)/\left(r_1^2 - r_2^2\right)\right] \quad (5)$$

where each length is shown to fig.2, k_a and k_r is thermal conductivities; the axial and radial. The core and magnet is described by these equation, on the other hand, coil and complex shape is described according to thermal flow.

2.2 Thermal resistance of the convection

The convection is caused in the air gap and housing surface. If heat is applied to fluid when a fluid is some surface or atmosphere, the fluids flow the surface due to difference of density. This is called natural convection. On the surface, motor temperature is increased, difference of density between high and low level is occurred. On the other hand, forced convection is caused by rotating rotor in the air gap. The natural and forced convection is determined by Taylor number (Ta) which is dimensionless number. (6) is Nusselt number (Nu) according to Ta [6].

$$\begin{cases} Nu = 2 & (Ta < 1700) \\ Nu = 0.128(Ta^2 / F_g^2)^{0.367} & (1700 < Ta^2 / F_g^2 < 10^4) \\ Nu = 0.409(Ta^2 / F_g^2)^{0.241} & (10^4 < Ta^2 / F_g^2 < 10^7) \end{cases} \quad (6)$$

On the housing, natural convection is occurred by motor loss. For obtaining the coefficient of natural convection, Nu must be determined. The calculation of Nu can be computed by the equation related to Rayleigh number (Ra) and Prantle number (Pr).

$$Nu = \left\{0.60 + \frac{0.387 Ra_D^{1/6}}{\left[1+(0.559/\mathrm{Pr})^{9/16}\right]^{8/27}}\right\}^2 \quad (7)$$

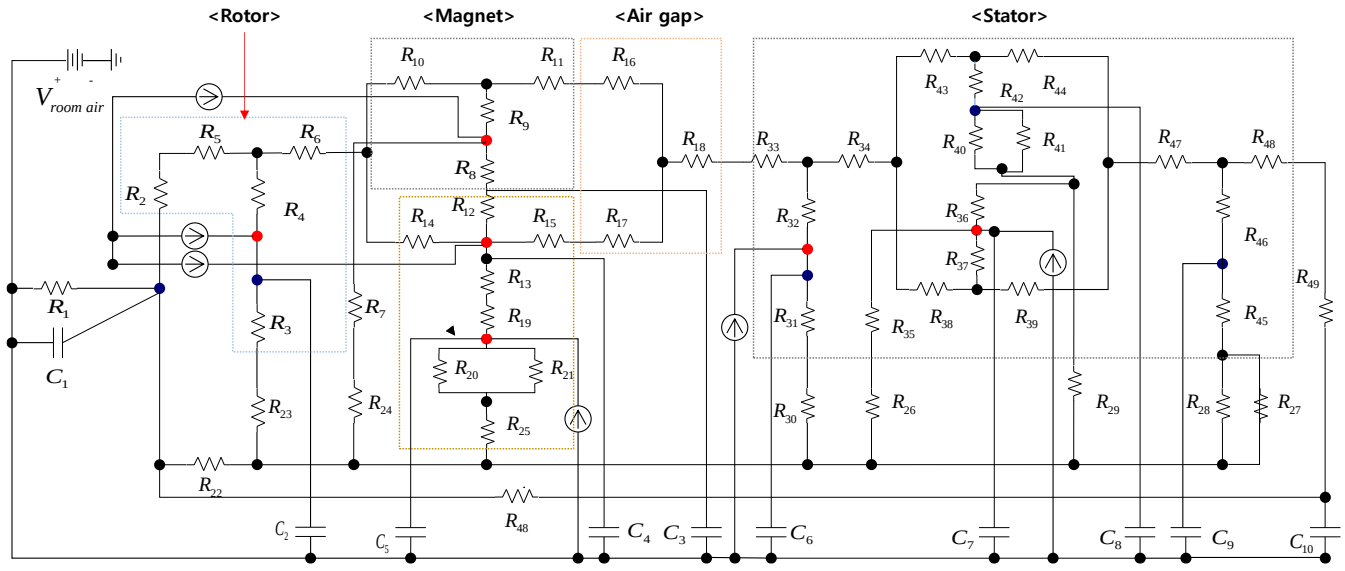

Figure 4: The configuration of the equivalent thermal circuit.

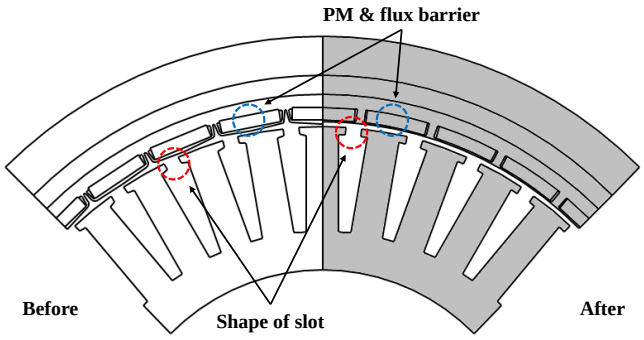

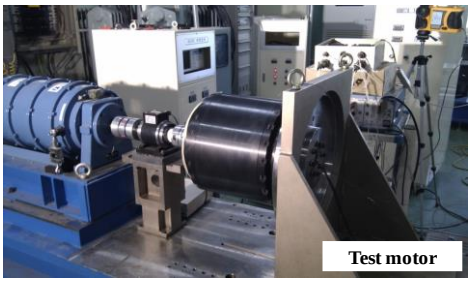

Figure 6: Test motor for thermal analysis.

	Unit	*Value*
Pole / Slot	-	32 / 36
DC link voltage	V_{DC}	680
Current limit	A_{rms}	-
Max. torque	*Nm*	1000
Output power	*kW*	1570
Max. speed	*rpm*	14.3
Operating temperature	^oC	-10 ~ 60

Table 1: Specification of test motor.

	Thermal conductivity *(W/m ^oC)*	*Specific heat* *(J/kg ^oC)*	*Density* *(kg/m^3)*
Core	49.8	502	7850
Housing	49.8	486	7850
Coil	394.0	486	8960
PM	9.0	440	7650

Table 2: Material specification.

Nu is computed by equation according to the type of thermal flow between natural and forced convection.
Coefficient of convective heat transfer is obtained by

$$h = \frac{Nu \cdot k}{L} \tag{8}$$

where h is coefficient of heat transfer, k is coefficient of conductive heat transfer, and L is area according to air flow. Therefore, resistance of convective heat transfer is derived by

$$R_{conv} = \frac{1}{hA} \tag{9}$$

where A is area to air flow.

2.3 Heat source

In the motor, heat source is composed by the copper loss, the core loss. The copper loss is winding loss which current flow through. The core loss is calculated by FEM, and fig. 3 shows the calculation process of core loss [7,8].

2.4 Thermal capacitance

Thermal capacity is necessary quantity which rise the 1^{o}C of the temperature of matter. This is expressed by

$$C_m = \rho_m V_m c \tag{10}$$

where C_m is thermal capacitance, ρ_m is density, V_m is each motor volume, and c is specific heat of material.

3 Thermal equivalent circuit

The thermal equivalent circuit network is shown in Fig. 4. This circuit is composed to resistance, heat source, and capacitance. Linear differential equation for the node i can be derived as expressed in (11) [6].

$$C_i \frac{dT_i}{dt} = \frac{1}{R_{ji}}(T_j - T_i) + g_i \tag{11}$$

where C_i is the i^{th} node thermal capacitance, T_i is the i^{th} node temperature, R_{ji} is thermal resistance between two adjacent nodes, i and j, and g_i is heat generation at node i.

4 Thermal analysis and result

4.1 Analysis model

Fig. 5 shows the analysis model which is composed equivalence model, left side is convert to right side. The test motor is 32pole/36slot. Table 1 shows the specification of test motor. The motor operated in 1000Nm and 14.3rpm. The material data is shown table 2.

4.2 Analysis and test result

The test is conducted under the 800Nm and 14.3rpm. This operating point is high torque and low speed, copper loss is very larger than core loss and eddy current loss of PM. Table

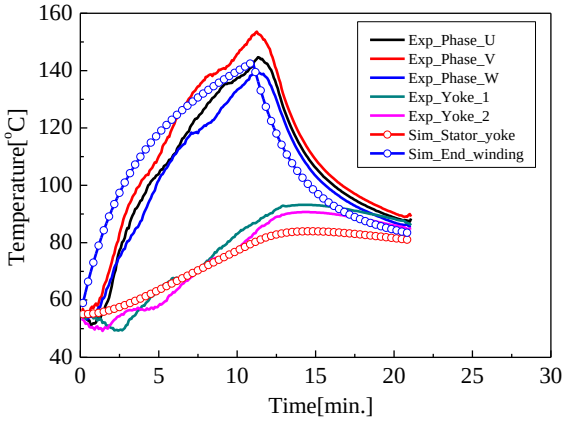

Figure 7: Analysis and test result @ 14.3rpm.

	Copper loss	*Core loss*		
		Yoke	*Teeth*	*Rotor*
Value (W)	1314.0	3.8	2.4	1.2

Table 3: Value of the heat source @14.3rpm.

	Analysis (°C)	*Test (°C)*	*Error(%)*
End winding	143.0	145.8	1.0
Stator yoke	79.9	84.8	6.1

Table 4: Analysis and test result

3 shows the loss of motor. This value cause the temperature rising.

The computed value of heat transfer coefficient is 20.1 W/m^2·°C in the surface and 26.3 W/m^2·°C in the air gap. These values are calculated by (6)-(8). The value in the air gap is low because motor is very low speed in the forced convection. Fig. 6 shows the test motor. The thermocouple is attached in end winding which is the hottest point, because the radiant heat is very low than stator winding. The heat of end winding is radiant by air which is low value. On the other hand, heat of stator winding is radiant by core in shape of conduction.

Fig. 7 and table 4 show the analysis and test result at 14.3rpm. The mean temperature of end winding, hottest point, rises at 145.8°C in the test. The analysis result is 143.0°C. The error between analysis and test is 6%. In addition the temperature curve is analogous in the changing of the time. These low error is cause by very low speed. In the high speed, the coefficient of convective heat transfer is difficult. In general, the error of this thermal equivalent circuit network 10-15%.

5 Conclusion

In this paper, temperature is estimated by using thermal equivalent circuit network. The parameter is obtained to dimensionless number and thermal equation. The thermal circuit is composed by equivalent thermal parameter. According to thermal test, thermal circuit is verified. Therefore, this circuit is can be an effective method to predict the motor temperature in the initial design.

Acknowledgements

This research was supported by the MSIP(Ministry of Science, ICT&Future Planning), Korea, under the C-ITRC(Convergence Information Technology Research Center) support program (NIPA-2013-H0401-13-1008) supervised by the NIPA(National IT Industry Promotion Agency)

References

[1] C. Feng, P. Yulong, L. Xinmei, G. Bin, and C. Shukang, "The Performance Research of Starter-Generator Based on Reluctance Torque Used in HEV," *IEEE Trans. on Magn.*, **volume** 45, no.1, pp. 635–638, (2009).

[2] J. Hur and B. W. Kim, "Rotor Shape Design of an Interior PM Type BLDC Motor for Improving Mechanical Vibration and EMI Characteristics," *JEET*, **volume** 5, no. 3, pp.462-467, (2010).

[3] V. Gnielinski, "New Equations for Heat and Mass Transfer in Turbulent Pipe and Channel Flow," *American Institute of Chemical Engineer*, **volume** 16, no. 3, pp. 359-368, (1961).

[4] Y. A. Cengel, *Heat transfer: A practical approach*, 2nd ed., McGraw-Hill, (2003).

[5] P. H. Mellor, D. R. Roberts, D. Turner, "Lumped Parameter Thermal Model For Electrical Machines of TEFC Design," *IEE*, **volume** 138, no. 5, (1991).

[6] B. H. Lee, K. S. Kim, J. W. Jung, J. P. Hong, and Y. K. Kim, "Temperature estimation of IPMSM using thermal equivalent circuit," *IEEE Trans. on Magn.*, **volume** 48, no.11, pp. 2949–2952, (2012).

[7] S. Adhikari, S. K. Halgamuge, and H. C. Watson, "An Online Power-Balancing Strategy for a Parallel Hybrid Electric Vehicle Assisted by an Integrated Starter Generator," *IEEE Trans. on Vehicular Technology*, **volume** 59, no.6, pp. 2689–2699, (2010).

[8] B. H. Lee, S. O Kwon, T. Sun, J. P. Hong, G. H. Lee, J. Hur, "Modeling of Core Loss Resistance for d-q Equivalent Circuit Analysis of IPMSM considering Harmonic Linkage Flux," *IEEE Trans. on Magn.*, **volume** 47, no.5, pp. 1066-1069, May, (2011).